Charm Physics With Polarized beams and Target at Jefferson Lab. 12 GeV

Z. Akbar*and D. Keller†

University of Virginia

June 10, 2019

Abstract

We present this Letter-of-Intent to measure various spin observables in the photoproduction of open charm and charmonium with an 11 GeV electron beam to determine the gluon density within the nucleon, investigate the charm-production mechanism near threshold and to do a high sensitivity search of the possible exotic states that include charm and anti-charm quarks. The experiment will be carried out in Hall C at Jefferson Lab, using the similar experimental set up as proposed in the approved PR12-17-008 proposal, which contains the Compact Photon Source, the Neutral Particle Spectrometer, the BigBite Spectrometer and the UVA/JLab-NH_3 polarized target. The coherent photon beams with circular and linear polarizations produced from the diamond radiator will be utilized along with the longitudinally-polarized target to extract several observables (A_{LL}, A_z, Σ and G) from the reactions: $\gamma p \rightarrow D\,X$, $\gamma p \rightarrow \bar{D}\Lambda_c^+$, $\gamma p \rightarrow \bar{D}\Sigma_c^+$ and $\gamma p \rightarrow J/\psi p$.

The asymmetry in the production of open charm, tagged by decays of D mesons is closely related to the polarized gluon spin density, $\Delta g(x)$. The high luminosity Jefferson Lab 12 GeV allows for studying the gluon distribution at high-x regimes which are completely unexplored. Polarization observables of the exclusive reactions $\gamma p \rightarrow \bar{D} + \Lambda_c^+(\Sigma_c^+)$ are essential to probe the charm particle dynamics at threshold and to investigate the existence of exotic states which are predicted to decay dominantly to $\Lambda_c^+\bar{D}$ and $\Sigma_c^+\bar{D}$. This experiment will also complements several proposals aiming to search for recently observed LHCb P_c^+ states and provide additional information from the polarization observables of $\gamma p \rightarrow J/\psi p$. We request a total of 20 days of data taking with the 11 GeV electron beam.

*Email: za2hd@virginia.edu

†Email: dustin@jlab.org

1 Introduction and Motivation

Charm physics covers the study of hadrons containing charm quarks and provides a lot of opportunities for probing the strong and weak interactions [1]. Open charm physics can shed light on how the proton spin is shared among its constituents [2]. The photoproduction of open charm is the most promising approach for studying the gluon contribution, ΔG, to the nucleon spin [3]. The associated open charm photoproduction also have intrinsic physical interest, in the understanding of charm particle electrodynamics [4]. A renewed interest in charm physics followed after the CERN press office announced the observation of the pentaquark particles [5]. The clear peak observed by the LHCb collaboration in the $J/\psi + p$ spectrum provided strong support for the existence of exotic states that include charm and anti-charm quarks.

Several experiments were devoted to the study of charm physics, but, up to now, the energy range where the data are available is still relatively far from threshold [6],[7],[8],[9],[10],[11]. With Jefferson Lab at 12 GeV, the photoproduction of charmed hadrons near threshold become possible [12]. The threshold regime of open charm and charmonium production provide a new window into multi-quark, gluonic, and hidden-color correlation of hadronic and nuclear wavefunctions in QCD[13]. More studies are needed in order to clarify the physics of charm photoproduction at threshold. Polarization phenomena will be essential to understand the open charm and charmonium reaction mechanism. This Letter-of-Intent is proposed to measure various spin observables of the photoproduction of open charm, associated charm, and J/ψ-meson.

1.1 The gluon spin distribution from the polarized open charm photoproduction

A major challenge of particle physics is to disentangle how the nucleon's spin is built up from its quark and gluon constituents,

$$\frac{1}{2} = \frac{1}{s}\Delta\Sigma + \Delta G + L_q + L_g, \tag{1}$$

where $\Delta\Sigma$ denotes the quarks spin contribution, ΔG is the gluon spin contribution, and $L_{q,g}$ are the quark and gluon orbital angular momentum contributions. The world average for $\Delta\Sigma$ is unexpectedly small, approximately 23% of the nucleon spin [14]. The missing part of the nucleon spin should be explained by the gluon and sea-quark spin and/or the angular momentum of the partons.

The gluon spin contribution, ΔG is the integral of the gluon helicity distribution, $\Delta g(x)$, i.e. $\Delta G = \int_0^1 \Delta g(x)dx$, where x is the momentum fraction of the gluon.

Information about the gluon helicity distribution can be obtained in semi-inclusive deep inelastic scattering or photoproduction by selecting hadronic final states signaling the participation of gluon in the production mechanism, such as the photon-gluon-fusion (PGF) [15]. This PGF process can be tagged by the observation of charmed particles in the final state. Experimentally, one has to

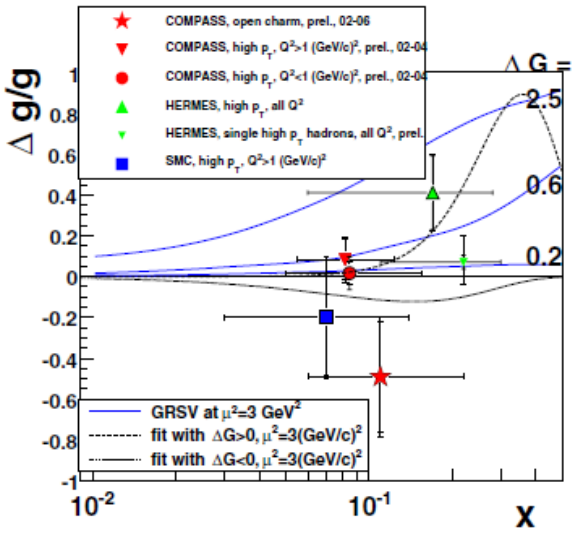

Figure 1: Comparison of the $\Delta g/g$ measurements from open charm and high P_T hadron production by COMPASS [15], SMC [16], and HERMES [17]. Image source [15].

measure a double helicity asymmetry, A_{LL} with a longitudinally polarized beam and target. This asymmetry is directly proportional to the polarization of gluon in the nucleon, $\frac{\Delta g(x)}{g(x)}$.

Figure 1 shows the results for $\frac{\Delta g(x)}{g(x)}$ from COMPASS [15], SMC [16], and HERMES [17]. The new results from COMPASS show reasonably small error bars and clearly favor a small value of $\frac{\Delta g(x)}{g(x)}$ at x around 0.1.

Gluon polarization within proton is also probed at RHIC through the measurements of A_{LL} in various channel involving gluon dominated hard scattering processes, such as inclusive π^0 and jet production channels [18]. Figure 2 shows the A_{LL} measurements from both channels by PHENIX and STAR experiments.

The experimental efforts for probing the gluon polarization have been dominated by the low-x regime. The high-x regime is under explored. Jefferson Lab with the new 12 GeV era puts the high-x physics as one of its major program.

Photoproduction of open charm through the process of photon-gluon-fusion (Figure 3) is the most promising approach for studying polarized gluon in the nucleon. The minimum x that is covered by this process depends on the photon energy,

$$x_{min} = \frac{4m_c^2}{2Mk}, \tag{2}$$

where M is the nucleon mass, m_c is the charm-quark mass of about 1.5 GeV,

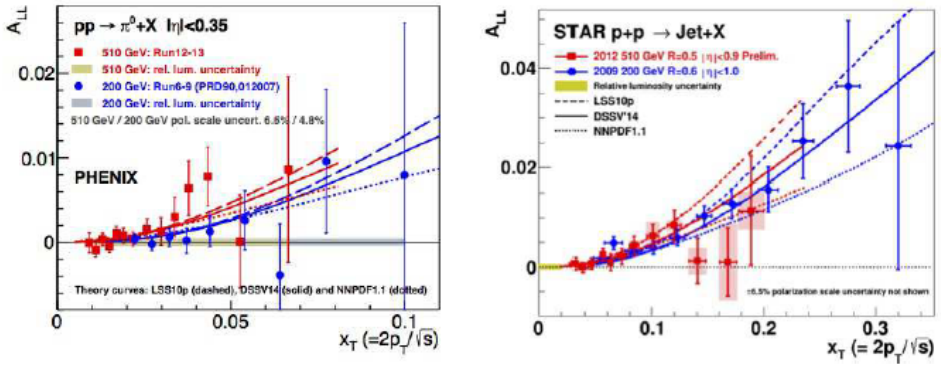

Figure 2: (left) A_{LL} vs x_T measurements from PHENIX for π^0 production in 200 GeV and 500 GeV c.m. energy. (right) A_{LL} vs x_T measurements from STAR for Jet production in 200 GeV and 500 GeV c.m. energy. Image source [18].

k is the photon energy. JLabs 12 GeV beam can allow kinematic coverage of $0.41 < x_{min} < 1$, which is completely unexplored.

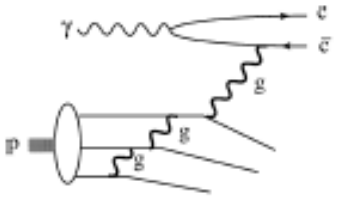

Figure 3: Photon-gluon-fusion process inside nucleon. Image source [13].

The spin-averaged of the cross section from the photon-gluon-fusion (PGF) process is given by an integral over the product of elementary PGF cross section $\sigma_{PGF}(\hat{s},\, \cos\theta)$ and the gluon distribution $g(x,\, Q^2)$ [3],

$$\sigma_{\gamma p} = \int_{x_{min}}^{1} g(x,\, Q^2) dx \int_{-1}^{1} \sigma_{PGF}(\hat{s},\, \cos\theta)\, \beta\, d\cos\theta, \tag{3}$$

where $\beta = \sqrt{1 - \frac{4m_c^2}{\hat{s}}}$, $\hat{s} = xs$ is the square of the c.m. energy in the photon-gluon system (or the $c\bar{c}$ system), $s = 2Mk + M^2$ is the square of the c.m. energy in the photon-nucleon system, θ is the c.m. angle of the charm quarks. Once the charm quarks are produced, they undergo the fragmentation process. D mesons (D^0, $\bar{D}^0$, D^+, D^-) are the most produced hadrons that resulted from this fragmentation.

For circularly-polarized photons and longitudinally-polarized nucleons, the difference in the cross section for two different helicity orientations (parallel and

anti-parallel) is

$$\Delta\sigma_{\gamma p} = \int_{x_{min}}^{1} \Delta g(x,\, Q^2) dx \int_{-1}^{1} \Delta\sigma_{PGF}(\hat{s},\, \cos\theta)\, \beta\, d\cos\theta. \tag{4}$$

We can define an experimental asymmetry

$$A_{LL} = \frac{1}{P_b P_t f} \frac{N^{\uparrow\uparrow} - N^{\uparrow\downarrow}}{N^{\uparrow\uparrow} + N^{\uparrow\downarrow}} = \frac{\Delta\sigma_{\gamma p}}{\sigma_{\gamma p}}, \tag{5}$$

where P_b is the beam polarization, P_t is the target polarization, f is the dilution factor. $N^{\uparrow\uparrow}$ and $N^{\uparrow\downarrow}$ denote the number of D mesons detected when the beam-target spin configuration are parallel and anti-parallel. Hence by measuring the asymmetry A_{LL}, we can extract the information about the gluon polarization in the nucleon. The major goal of this Letter-of-Intent is to suggest the A_{LL} measurement from the open charm photoproduction tagged by the D mesons produced using circularly-polarized photons and longitudinally-polarized protons for high-x region.

1.2 Polarization observables in exclusive open charm photoproduction process

The experiments aiming to measure the gluon polarization from the photon-gluon-fusion process ideally isolate c and $\bar{c}$ from target fragments, and so unaffected by the polarization of the target remnants. This is the case in the limit of very high photon energy but not at threshold. At our energy the hadronization process includes some coupling between the charmed quarks and the target quarks. This process as shown in Figure 4 and is the associated production. The observed excess of $\bar{D}$ mesons over D mesons and the excess of Λ_c over $\bar{\Lambda_c}$ are evidence for associated production. The $\bar{D}$ and $\bar{\Lambda_c}$ can be produced from the quark and diquark from the target (as shown in figure 4), while the D and $\bar{\Lambda_c}$ cannot be.

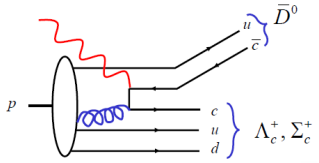

Figure 4: Associated and exclusive open charm production in $\gamma p \rightarrow \bar{D} + \Lambda_c^+(\Sigma_c^+)$. Image source [12].

We plan to tag the open charm photoproduction with the produced D and $\bar{D}$ mesons from the photon-gluon-fusion process. The associated production will be the primary background in the measurement of the gluon polarization. Hence, we need to quantify and exclude the contributions from exclusive and associated production of $\gamma p \rightarrow \bar{D} + \Lambda_c^+(\Sigma_c^+)$.

The exclusive reaction, $\gamma p \rightarrow \bar{D} + \Lambda_c^+(\Sigma_c^+)$, which are the objects of this Letter-of-Intent, are important not only as the backgrounds for the gluon-polarization measurement, but also to understand the charm particle dynamics, especially at threshold. The photoproduction of $\bar{D}\Lambda_c(\Sigma_c)$ can be used to study the electromagnetic properties of charmed particles, such as the magnetic moments of Y_c hyperons and the transition magnetic moment ($g_{D^*D\gamma}$ and $g_{D^{*+}D\gamma}$), which are not well known. These channels are also important to test the $SU(4)$-symmetry for the strong NDY_c-coupling constants. The strong coupling constants which enter in the calculation of the observables are connected to corresponding constants for strange particle production if the $SU(4)$-symmetry is valid.

Tomasi-Gustafsson and Rekalo [4], use the effective Lagrangian approach to calculate the differential cross section and polarization observables for the reactions $\gamma p \rightarrow \bar{D} + \Lambda_c^+$, $\gamma p \rightarrow \bar{D} + \Sigma_c^+$, and $\gamma p \rightarrow D^- + \Sigma_c^{++}$. Various reaction mechanism, such as, the associated photon-gluon-fusion, the diffractive production, quark and antiquark annihilation, and mesons and baryons exchange are taken into account (see Figure 5).

Figure 6 shows the differential cross section and various polarization observables predictions by Tomasi-Gustafsson and Rekalo for the reactions $\gamma p \rightarrow \bar{D} + \Lambda_c^+$, $\gamma p \rightarrow \bar{D} + \Sigma_c^+$, and $\gamma p \rightarrow D^- + \Sigma_c^{++}$.

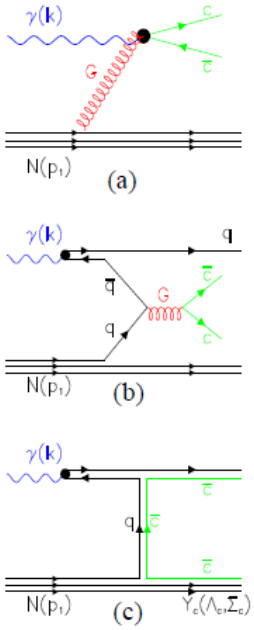

Figure 5: Feynman diagrams for associated open charm photoproduction: (a) photon-gluon fusion; (b) $q\bar{q}$ annihilation; (c) t-channel meson exchange. Image source [4].

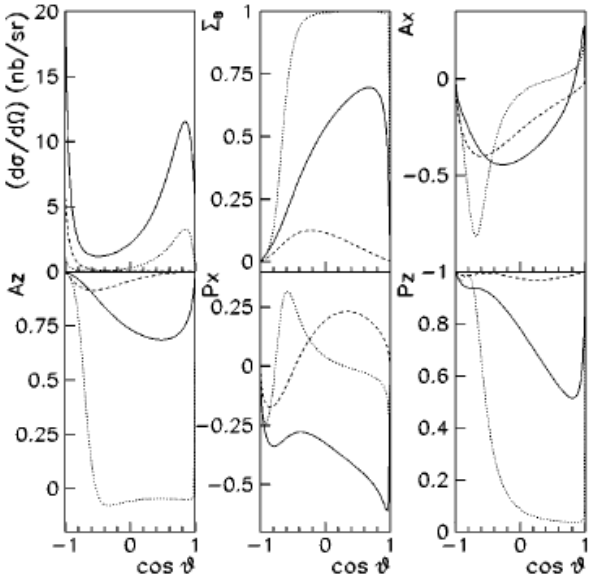

Figure 6: Tomasi-Gustafsson and Rekalo predictions on the differential cross section and polarization observables Σ_B, A_x, A_z, P_x and P_z for the reactions: $\gamma p \to \bar{D} + \Lambda_c^+$ (solid lines), $\gamma p \to \bar{D} + \Sigma_c^+$ (dotted lines), and $\gamma p \to D^- + \Sigma_c^{++}$ (dashed lines). This model does not take into account the presence of s-channel pentaquark states. Image source [4].

The exclusive channels of $\gamma p \to \bar{D} + \Lambda_c^+(\Sigma_c^+)$ also open up a new window into the pentaquark search. In 2015, the LHCb collaboration observed two resonances, $P_c(4380)$ and $P_c(4450)$ in the pJ/ψ invariant mass spectrum from the $\Lambda_b \to J/\psi K^- p$ decays [5]. These resonances indicate that they have a minimal quark content of $uudc\bar{c}$. Recently, the LHCb collaboration found that the $P_c(4450)$ is actually composed of two narrow resonances, $P_c(4440)$ and $P_c(4457)$ [19]. They also observed a new state, $P_c(4312)$. A lot of theoretical papers appeared following the announcement with various interpretations of the observed resonance, such as a true pentaquark state, a bound state of charmonium and proton, or a meson-baryon molecule.

X. Z. Weng et al. studied the mass spectrum of the hidden charm pentaquark in the framework of an extended chromomagnetic model [20]. They predicted a pentaquark state, $P_c(4372.4)$ with $I, J^P = \frac{1}{2}, \frac{1}{2}^-$ and decays dominantly to $\Lambda_c \bar{D}$. They also found a pentaquark state, $P_c(4327.0)$ with $I, J^P = \frac{1}{2}, \frac{1}{2}^-$ that decays dominantly to $\Sigma_c \bar{D}$. Figure 8 shows the mass spectra prediction of the $qqqc\bar{c}$ pentaquark states for $I = \frac{1}{2}, \frac{3}{2}$ and table 1 shows the partial width ratios for the open charm decays of the pentaquark states.

Probing the existence and nature of the pentaquark states with minimal ambiguity requires additional information from the polarization observables. The scattering amplitudes from various contributing processes are entangled with

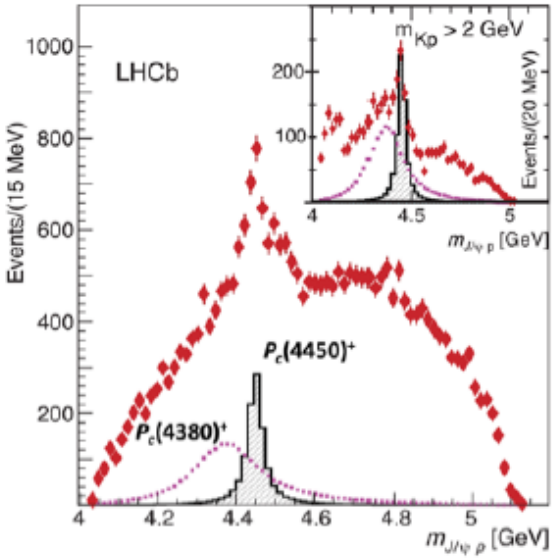

Figure 7: The invariant mass of $J/\psi p$ from $\Lambda_b \to J/\psi p K$, from LHCb. Image source [21].

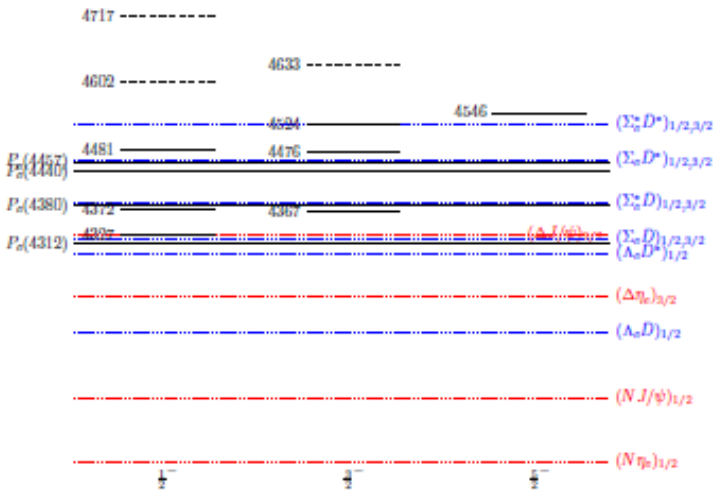

Figure 8: Mass spectra of the $qqqc\bar{c}$ pentaquark states. The $I = \frac{1}{2}(\frac{3}{2})$ are denoted by solid (dashed) lines. The dotted lines indicate various meson-baryon thresholds. Image source [20].

each other. The unpolarized cross section only gives information on the magnitude of the amplitudes which often leads to ambiguous solutions for the resonant contributions. The polarization observables are sensitive to the presence of resonant states and large changes in these observables can result when approaching a Wigner cusp. Information on the spin correlations add considerably to the discrimination between models. Predictions for these types of observables and the expected enhancements from various contributions can be use to measure properties of exotics and deviations near the charm threshold. Using the premise of analyticity and unitarity it is possible to explore the changes in the full set of target helicity correlations in photon-proton scattering, A_{LL}, A_{LS}, A_{LN} as well as A_{NN} for a set of assumed quantum numbers in the resonance formation. These observables can have different name depending on convention.

I	J^P	Mass	$\Delta J/\psi$	$\Delta\eta_c$	NJ/ψ	$N\eta_c$
$\frac{3}{2}$	$\frac{1}{2}^-$	4601.9	1			
		4717.1	1			
	$\frac{3}{2}^-$	4633.0	1	5.5		
$\frac{1}{2}$	$\frac{1}{2}^-$	4327.0			1	3.0
		4372.4			1	0.8
		4480.9			1	0.3
	$\frac{3}{2}^-$	4367.4			1	
		4476.3			1	
		4524.5			1	
	$\frac{5}{2}^-$	4546.0				

I	J^P	Mass	$\Sigma_c^*\bar{D}^*$	$\Sigma_c^*\bar{D}$	$\Sigma_c\bar{D}^*$	$\Sigma_c\bar{D}$	$\Lambda_c\bar{D}^*$	$\Lambda_c\bar{D}$
$\frac{3}{2}$	$\frac{1}{2}^-$	4601.9	0.05		1	0.4		
		4717.1	7.0		1	0.2		
	$\frac{3}{2}^-$	4633.0	5.3	3.1	1			
$\frac{1}{2}$	$\frac{1}{2}^-$	4327.0	0		0	1.3	1	0.02
		4372.4	0		0	0.7	1	57.6
		4480.9	0		0.3	0.09	1	0.07
	$\frac{3}{2}^-$	4367.4	0	0	0		1	
		4476.3	0	0.2	1.9		1	
		4524.5	0	0.58	0.63		1	
	$\frac{5}{2}^-$	4546.0	1					

Table 1: The partial width ratios for the charmed particle decays of the pentaquark states. For each state, one mode is used as the reference channel, and the partial width ratios of other channels are calculated relative to this channel. The mass are all in MeV. Table source [20]

We intend to measure different polarization observables for the exclusive $\gamma p \to \bar{D} + \Lambda_c^+(\Sigma_c^+)$ reactions, starting from the one-spin asymmetry Σ_B, induced by linearly-polarized photons

$$\Sigma_B = \frac{d\sigma_\perp/d\Omega - d\sigma_\parallel/\Omega}{d\sigma_\perp/d\Omega + d\sigma_\parallel/\Omega}, \tag{6}$$

where $d\sigma_\perp/d\Omega$ and $d\sigma_\parallel/d\Omega$ are the differential cross section for the linearly-polarized photon, which is orthogonal and parallel to the reaction plane. Linearly-polarized photons allow one to distinguish between natural and unnatural parity exchange.

We also consider gaining additional information using circularly-polarized photon beams and longitudinally-polarized target. The $\gamma p \to \bar{D} + \Lambda_c^+(\Sigma_c^+)$ cross sections with circularly-polarized photon beams and longitudinally-polarized target are described by two different asymmetries

$$d\sigma/d\Omega = d\sigma_0/d\Omega\,(1 - \lambda T_x A_x - \lambda T_z A_z), \tag{7}$$

where $\lambda = \pm 1$ is the photon helicity, T_x and T_z are the components of the proton polarization $\vec{T}$, $d\sigma_0/d\Omega$ is the unpolarized cross section.

It may be possible to isolate the contribution of pentaquark candidate decays to $\bar{D} + \Lambda_c^+(\Sigma_c^+)$ as shown in Figure 9. This assumes the other production mechanisms are also taken into account, for example, the associated photon-gluon-fusion, the diffractive production, quark and antiquark annihilation, and mesons and baryons exchange (see figure 5).

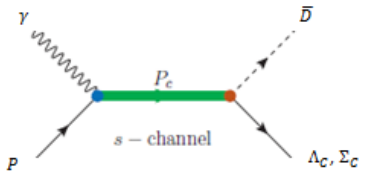

Figure 9: The s-channel resonant production of $\bar{D} + \Lambda_c^+(\Sigma_c^+)$ through a pentaquark state. Image source [23].

The overlapping nature of the (predicted) pentaquark states makes it impossible to simply go "peak hunting" for their identification. However, the quantum numbers of each nucleon resonance determines the angular distribution of its decay products. Thus, by measuring these decay distributions, it is possible to identify nucleon resonance states. This is the standard technique of Partial Wave Analysis (PWA). With the suggested measurement it will be possible to measure the observables of Σ_B and A_z for the $\gamma p \to \bar{D} + \Lambda_c^+$ and $\gamma p \to \bar{D} + \Sigma_c^+$. These measurements will be the first of their kind and could be used as inputs to a PWA and as a probe to the nature of pentaquarks candidates.

1.3 Polarization observables in $\gamma p \to J/\psi p$ reaction

As we mentioned before that the discovery of the LHCb-pentaquarks was received with excitement by the physics community. But the resonance states can not be unambiguously identified as exotic pentaquarks without further experimental measurements. Several experiments have been proposed at Jefferson Lab to study these exotic states. The experiments are proposed in Hall A [21], B [22], and C [23]. Our suggested project is complementary to those proposed experiments, which plan to measure the cross section in Hall B and Hall C and the polarization observables (A_{LL} and K_{LL}) using circularly-polarized photons and longitudinally-polarized target in Hall A.

The J/ψ is a vector meson. A complete description of vector meson photoproduction requires 24 complex helicity amplitudes. Two helicities are form the beam, two form the target, three form the vector meson and two form the recoil proton, amounting to a total of $2 \times 2 \times 3 \times 2 = 24$ scattering amplitudes. However, parity invariance reduces the number of independent amplitudes to 12. This implies that we need to perform many different experiments to fully constrain the 23 independent real numbers needed to completely describe the

reaction $\gamma p \rightarrow pV$ (V is a vector meson), where the overall phase is irrelevant. These scattering amplitudes are embedded in the cross section and the mentioned polarization observables.

For the reaction $\gamma p \rightarrow pV$, when only the beam and target polarization are measured, the differential cross section reduces to the form [24]:

$$\frac{d\sigma}{dx_i} = \sigma_0 \Big(1 - \delta_l \mathbf{\Sigma} \cos 2\beta + \Lambda_x(-\delta_l \mathbf{H} \sin 2\beta + \delta_\odot \mathbf{F}) - \Lambda_y(-\mathbf{T} + \delta_l \mathbf{P} \cos 2\beta) - \Lambda_z(-\delta_l \mathbf{G} \sin 2\beta + \delta_\odot \mathbf{E}) \Big), \tag{8}$$

where x_i are the kinematic variables and $\delta_l(\delta_\odot)$ denote the degree of linear (circular) polarization of the beam. Λ_x, Λ_y and Λ_z are the components of the target polarizations with respect to the reaction plane. The angle β denotes the angle between the direction of the linearly-polarized photon beam and the reaction plane. σ_0 is the cross section, which is associated with the likelihood of scattering when both the target and beam are unpolarized. $(\Sigma, \mathbf{T})$, and $(\mathbf{H}, \mathbf{F}, \mathbf{P}, \mathbf{G}, \mathbf{E})$ are the single and double polarization observables.

There are also polarization observables associated with the decay distribution of the vector meson called the Spin Density Matrix Elements (SDMEs). A density matrix is a matrix that describes a quantum system in a mixed state, a statistical ensemble of several quantum states. If the density matrix for a particle is known, then all quantum mechanical observables can be calculated. The SDMEs of a vector meson then refer to the density of the vector meson's spin projections. For a particle with n states, in a given basis, each having wave function ψ, the density matrix is

$$\rho = \sum_{ij}^{n} a_{ij} \psi_j \psi_i. \tag{9}$$

Diagonal elements of the matrix, a_{ii}, represent the probability that the particle is in state ψ_i. Thus, the decay angular distribution of the vector meson in its rest frame can be constructed using the density matrix as

$$\frac{\mathrm{d}N}{\mathrm{d}\cos\theta \mathrm{d}\phi} = M\rho(V)M^\dagger, \tag{10}$$

where M is the decay amplitude and $\rho(V)$ is the spin density matrix of the vector meson. The exact form of the SDME were derived by K. Schilling *et al* [25]. The information gathered form our suggest experiment can be used towards initial measurements of the spin density matrix of the J/ψ.

We propose to measure two polarization observables: the beam asymmetry ($\mathbf{\Sigma}$) using linearly polarized photons and the $\mathbf{G}$ observable using the linearly polarized photons and longitudinally polarized target. These observables are complement to A_{LL} and K_{LL} which proposed to be measured in Hall A [21].

X. Y. Wang et al. investigated the production of pentaquark states $P_c(4312)$, $P_c(4440)$ and $P_c(4457)$ via s- channel in the $\gamma p \rightarrow J/\psi p$ reaction within the

framework of the effective Lagrangian approach and Vector Meson Dominance model [26]. The basic Feynman diagrams used in the calculation are shown in Figure 10 where the P_c candidates are produced through s- and u- channels and the t-channel pomeron exchange contribute as the background. The predictions of the beam asymmetry $\mathbf{\Sigma}$ for the $\gamma p \to J/\psi p$ at different energies near threshold are shown in Figure 11.

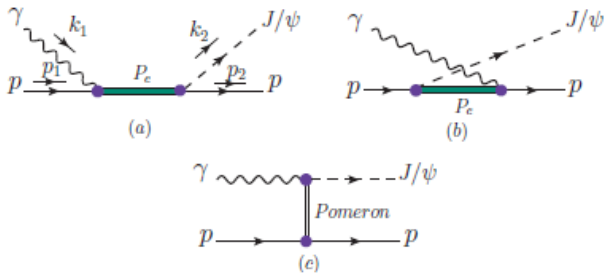

Figure 10: The production mechanisms of $\gamma p \to J/\psi p$ used in the model: (a) s-channel P_c production (b) u-channel P_c production (c) t-channel pomeron exchange. image source [26].

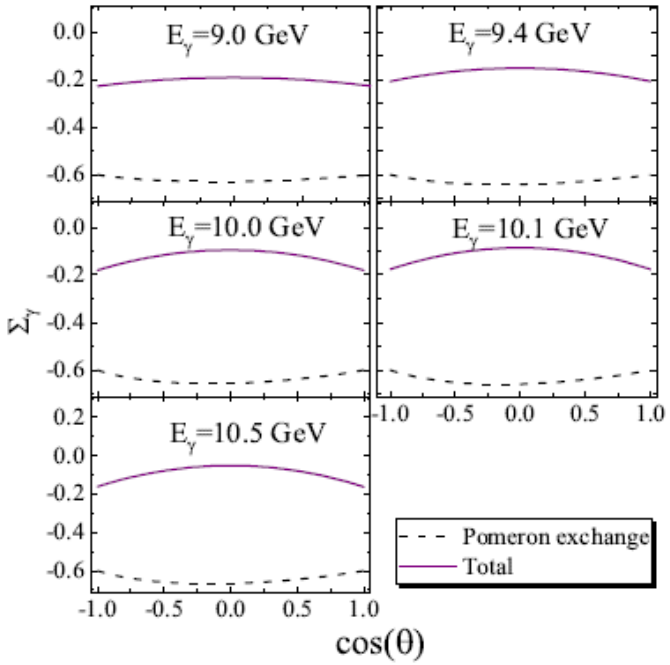

Figure 11: The beam asymmetry $\mathbf{\Sigma}$ of the $\gamma p \rightarrow J/\psi p$ reaction at $E_\gamma = 9.0 - 10.5$ GeV. Image source [26].

1.4 Summary

We plan to study the charm physics photoproduction near threshold by measuring various spin observables in the open charm photoproduction (tagged by the D mesons) and the exclusive $\gamma p \rightarrow \bar{D} + \Lambda_c^+$, $\gamma p \rightarrow \bar{D} + \Sigma_c^+$ and $\gamma p \rightarrow J/\psi p$ reactions.

The open charm photoproduction (tagged by the D mesons) with circularly-polarized photons and longitudinally-polarized target provide access to the gluon polarization in the nucleon, $\frac{\Delta g(x)}{g(x)}$. We also want to understand the threshold regime of charm production through the measurements of the spin observables in three exclusive channels ($\gamma p \rightarrow \bar{D} + \Lambda_c^+$, $\gamma p \rightarrow \bar{D} + \Sigma_c^+$ and $\gamma p \rightarrow J/\psi p$). These channels open up a new window into the (possible) pentaquark states. Polarization observables are very helpful to obtain the definite evidence for the pentaquark states and their nature. Table 1.4 shows the polarization observables measured for each reaction of interest and the configuration of the beam and target polarization.

Table 2: The polarization observables measured for each reaction of interest

Photon polarization	Target polarization	Reaction	Observables
Circular	Longitudinal	$\gamma p \rightarrow D + X$	A_{LL}
		$\gamma p \rightarrow \bar{D} + \Lambda_c^+$	A_z
		$\gamma p \rightarrow \bar{D} + \Sigma_c^+$	A_z
Linear	Unpolarized	$\gamma p \rightarrow \bar{D} + \Lambda_c^+$	Σ
		$\gamma p \rightarrow \bar{D} + \Sigma_c^+$	Σ
		$\gamma p \rightarrow J/\psi p$	Σ
Linear	Longitudinal	$\gamma p \rightarrow J/\psi$	G

2 Experimental Setup

The proposed experiment will take advantage of the experimental setup that was already approved in Hall C (PR12-17-008) [27], which utilize the Neutral Particle Spectrometer (NPS), The BigBite Spectrometer, the polarized NH_3 target and the Compact Photon Source as illustrated in Figure 12.

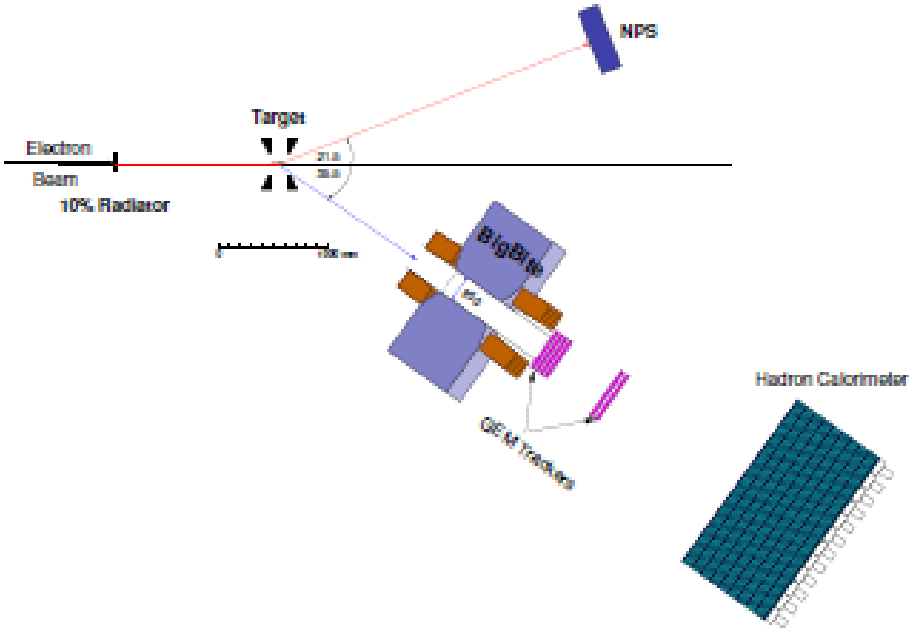

Figure 12: Schematic of the experimental setup as proposed in PR12-17-008. Image source [27].

Two major modifications are needed to carry out the proposed experiment. First, we will utilize diamond radiator instead of Cu to produce a coherent bremsstrahlung. Second, the NPS and the BigBite spectrometer will be placed at different range of angles to maximize the acceptance.

2.1 The Photon Source

The experimental program laid out in the PR12-17-008 proposal requires a real and high intensity photon source with sufficiently low radiation in the target and spectrometer area during operation. A device is developed to achieve ten times the luminosity while keeping the heat load on the target as well as the radiation level in the hall at acceptable levels. This device, a Compact Photon Source, will act as a combination of a sweeper magnet and a beam dump, and producing a narrow intense pure photon beam. The principal component of the Compact

Photon Source are: a conducting dipole magnet providing a strong horizontal field to sweep down the beam electrons, A 150-cm long W/Cu block with a set of 2-mm channels located in the dipole field which serves as a diffuser-absorber of an electromagnetic shower, a thick layer of heavy radiation shielding.

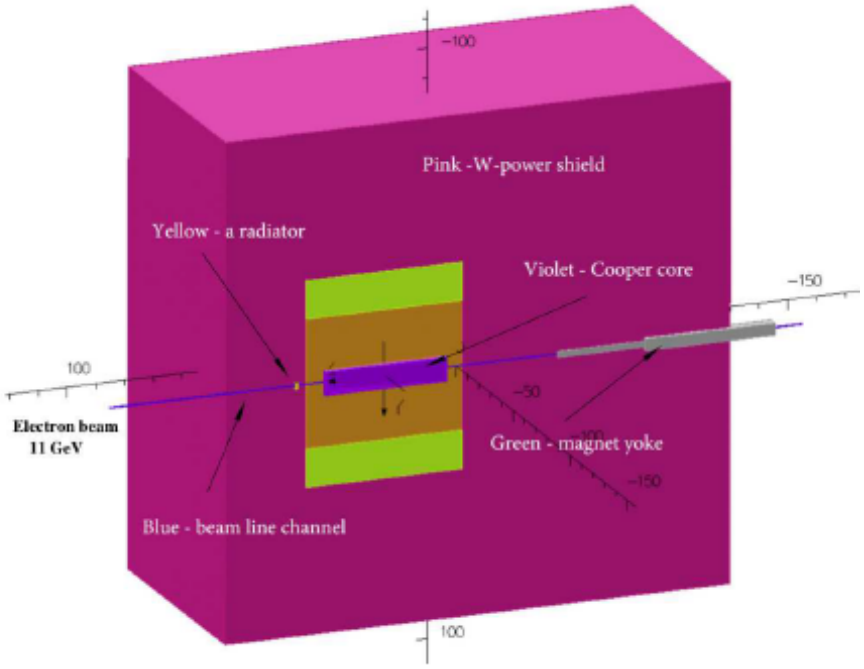

Figure 13: Schematic of the Compact Photon Source which provide a 1.5 T horizontal field to sweep the electrons down to the beam dump. Image source [28].

The major difference between our proposal and the approved PR12-17-008 proposal is the way photon beams are produced. Instead of using a copper radiator with 10% radiation length, we will use the diamond radiator to produce a coherent-bremsstrahlung photon beams.

J. D. Kellie et al. did a study on the selection and performance of diamond radiators used in coherent bremsstrahlung experiments at Mainz MAMI-B facility and the 12 GeV Jefferson Lab [29]. They concluded that a reasonable upper limit at 12 GeV Jefferson Lab. for which the spreading of the coherent peak and the reduction in the polarization are small requires a diamond of thickness $\sim 40\,\mu$m, which is 3.6×10^{-4} radiation length. The level of damage in the radiator for 12 GeV electron beam is also estimated, and the beam current of $3\,\mu$A could run for ~ 1 month at a full intensity before the diamond would experience radiation damage. Hence, the beam current at $2.5\,\mu$A will be used as in the PR12-17-008 proposal. The diamond orientation will be set up by a high precision goniometer to set the coherent peak up at 10 GeV.

2.2 The BigBite Spectrometer

The BigBite spectrometer is a large and non-focusing magnetic spectrometer, which has been used in many different experiments at 6 GeV Jefferson Lab. era. The GEM trackers are then developed as part of the 12 GeV upgrade to enable detection of high momentum particles. The momentum resolution of the new trackers is approximately 5%. A Hadron Calorimater (HCAL) is planned to be installed in addition to the GEM detectors.

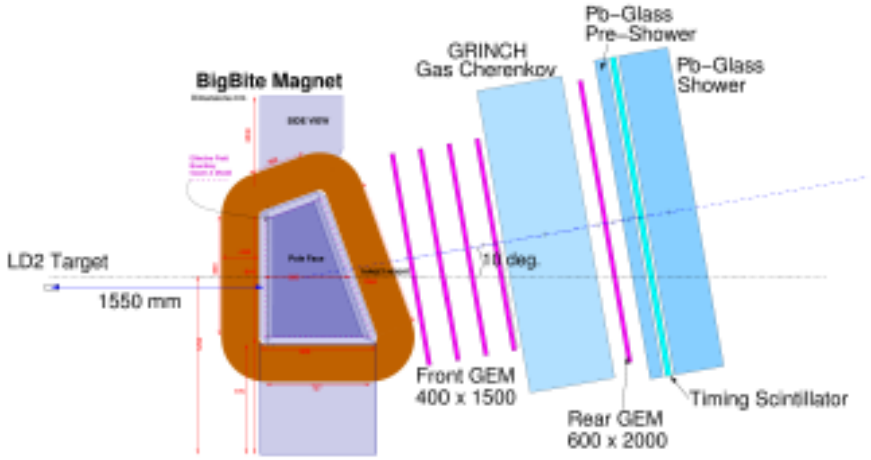

Figure 14: The BigBite spectrometer which set up as an electron spectrometer in this particular configuration. In our propesed experiment, the GRINCH, timing scintillators and shower counters will be replaced by a Hadron Calorimeter (HCAL). Image source [27].

2.3 The Neutral Particle Spectrometer

The Neutral Particle Spectrometer (NPS) is a $PbWO_4$-based electromagnetic calorimater capable of detecting high energy photons and leptons. The NPS provides good energy and spatial resolution in a high rate environment. The energy resolution is better than 3% and the position resolution is 3 mm. We will use the NPS to detect the leptons produced from the J/ψ decays.

2.4 The Polarized NH_3 Target

This experiment will also use the same NH_3-UVA/JLab target as proposed in the approved PR12-17-008 proposal. The target polarization will be oriented longitudinal to the beam. The Dynamic Nuclear Polarization (DNP) technique, which based on the 140 GHz microwaves to drive the hyperfine transitions is

applied to produces proton polarizations of up to 95%. The target cells are placed in a high (5 T) uniform magnetic field and low temperature (1 K). The low temperatures of the target is maintained by a high cooling power evaporation refrigerator.

The unique combination of high photon intensity and polarized target system optimizes the experimental statistical significance with respect to the target maintenance overhead. The rotating raster target system required for such an interface has already been demonstration at UVA and continues to be part of the ongoing RD to optimize this technology for a series of JLab experiment with a similar configuration to run in Hall C.

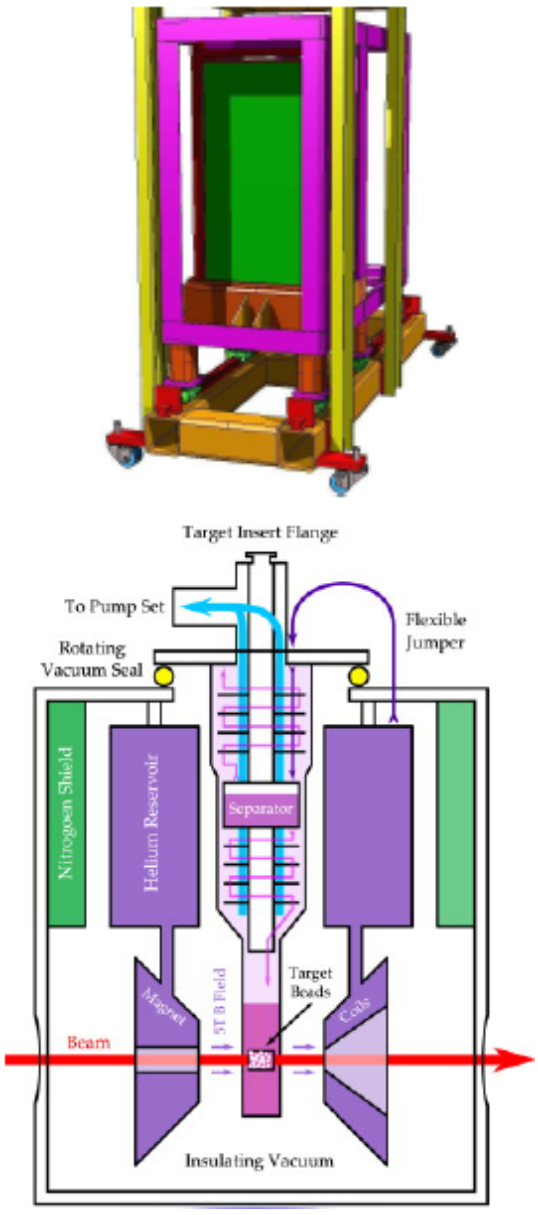

Figure 15: (Top) The Neutral Particle Spectrometer. (Bottom) The cross-sectional view of the polarized target. Image source [27].

3 Rate Estimations

In this section we will project the event rate of the processes, estimate the acceptance and describe the simulations.

3.1 $\gamma p \to \bar{D}\Lambda_c^+$ reaction

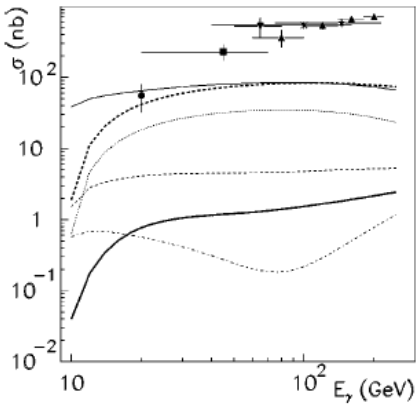

Figure 16: E_γ-dependence of the predicted total cross-sections for various charmed particle photoproduction reactions. The curves correspond to different reactions: $\gamma p \to \bar{D}\Lambda_c^+$ (solid line), $\gamma p \to D^-\Sigma_c^{++}$ (dashed line), $\gamma p \to \bar{D}\Sigma_c^+$ (dotted line). The other three curves correspond to the photoproduction with the neutron target. Image source [4].

The event rate of the process $\gamma p \to \bar{D}\Lambda_c^+$ (N) are the product of the cross section (σ), the photon flux (N_γ), the branching ratio (B_r), the detector acceptance (ϵ), and the target factors, which include the target density (ρ), the target length (l), the target atomic weight (A), and the Avogadro constant (N_A).

$$N = \sigma N_\gamma B_r \epsilon \frac{\rho l N_A}{A}. \tag{11}$$

The cross section of the open charm productions at threshold are experimentally unknown, but theoretically calculated by Tomasi-Gustafsson and Rekalo using the effective Lagrangian approach [4]. Figure 16 shows the calculated total cross sections as a function of E_γ for various photoproduction of charmed particles. The curves correspond to different reactions: $\gamma p \to \bar{D}\Lambda_c^+$ (solid line), $\gamma p \to D^-\Sigma_c^{++}$ (dashed line), $\gamma p \to \bar{D}\Sigma_c^+$ (dotted line). The other three curves correspond to the photoproduction with the neutron target.

The predicted cross section for the $\gamma p \to \bar{D}\Lambda_c^+$ reaction at threshold as shown in Figure 16 is approximately 30 nb. The total branching ratio for the exclusive decay $\bar{D} \to K^+\pi^-$ and $\Lambda_c^+ \to pK^-\pi^+$ is 0.19 %. The photon flux

is $6.2 \times 10^{11}\, s^{-1}$ or 5.4×10^{16} /day. Based on the equation 11 above, we can calculate the expected of event rates per day

$$N_{\bar{D}\Lambda_c^+} = 3 \times 10^5\, \epsilon. \tag{12}$$

The $\gamma p \rightarrow \bar{D}\Lambda_c^+ \rightarrow pKK\pi\pi$ simulated events are pure phase-space generated to estimate the acceptance (ϵ). Figure 17 shows the angular distributions (θ) of some particles in the final states: p, π^-, π^+, K^-.

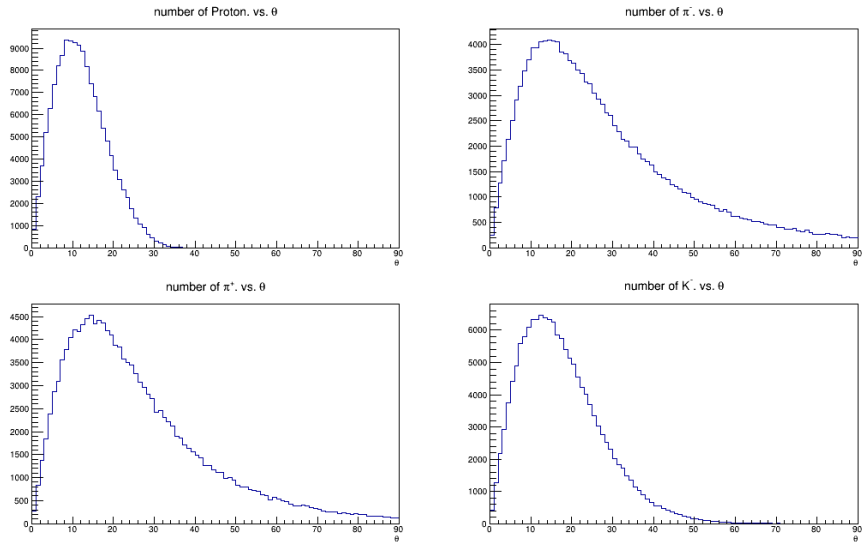

Figure 17: The angular distributions (θ) for some particles in the final states: (Top left) Proton, (Top right) π^-, (Bottom left) π^+ and (Bottom right) K^-.

We only use the BigBite spectrometer for the reaction $\gamma p \rightarrow \bar{D}\Lambda_c^+$. Hence, we require detection of either K^+ and π^- ($\bar{D} \rightarrow K^+\pi^-$) or p, K and π^+ ($\Lambda_c^+ \rightarrow pK^-\pi^+$) in the BigBite spectrometer. Therefore, we need to exclusively detect the decay products of the $\bar{D}$ or the Λ_c^+ so we then can apply kinematic constraints to the undetected meson/baryon. These constraints must assume a dominate peak energy from the coherent photon beam. The missing mass spectrum is then studies assuming an incoming photon energy at the dominant peak.

Based on the figure 17 above we found that the Bigbite provides the maximum acceptance if the spectrometer cover a range of angles between 10.4° and 26.5°.

The event rates per day is $3 \times 10^5\, \epsilon$ /day, where ϵ is the detector acceptance. We then generated 3×10^5 $\gamma p \rightarrow \bar{D}\Lambda_c^+$ events and counted the number of events that fall in the range of angles covered by the BigBite spectrometer for two different topologies:

1. K^+ and π^- are detected in the BigBite spectrometer ($\bar{D} \rightarrow K^+\pi^-$) and cut around Λ_c^+ is applied. 3756 events are obtained from this topology.

2. p, K^- and π^+ are detected in the BigBite spectrometer ($\Lambda_c^+ \rightarrow pK^-\pi^+$) and cut around $\bar{D}$ is applied. 1596 events are obtained from this topology.

Therefore, with the photon flux of $6.2 \times 10^{11}\,\gamma\mathrm{s}^{-1}$ and the acceptance of approximately 0.02% the resulting rate of detected $\gamma p \rightarrow \bar{D}\Lambda_c^+$ events is 5352 per day.

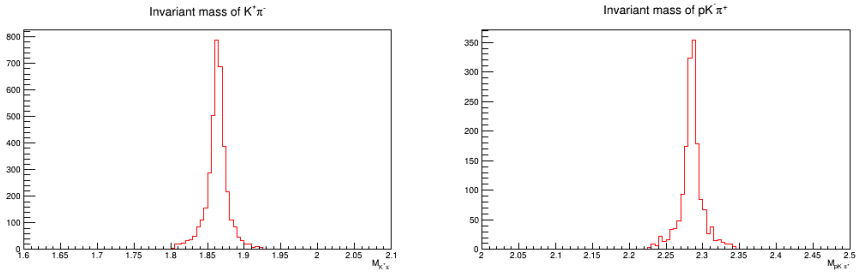

Figure 18: The events yield from two different topologies: (Left) 3756 events per day are obtained when K^+ and π^- are detected in the BigBite spectrometer ($\bar{D} \rightarrow K^+\pi^-$) and cut around Λ_c^+ mass is applied. (Right) 1586 are obtained when K^- and π^+ are detected in the BigBite spectrometer ($\Lambda_c^+ \rightarrow pK^-\pi^+$) and cut around $\bar{D}$ mass is applied.

As a preliminary study of the background, the $\gamma p \rightarrow pKK\pi\pi$ phase space events are generated statistics that are ten times larger than the generated $\gamma p \rightarrow \Lambda_c^+ D \rightarrow pKK\pi\pi$. Both channels are generated with the coherent photon distributions. Figure 19 shows the invariant mass of $K^+\pi^-$ (left) and the reconstructed missing Λ_c^+ (right) using the suggested analysis. The Λ_c^+ peak is broad as expected since the photons are untagged but still visible enough to impose the required kinematic constraint. We expect a full multivariate analysis will be advantageous to minimize the dilution factor and optimize the pseudo-exclusivity of each channel.

3.2 $\gamma p \rightarrow \bar{D}\Sigma_c^+$ reaction

The cross section of the $\gamma p \rightarrow \bar{D}\Sigma_c^+$ reaction at threshold is predicted by Tomasi-Gustafsson and Rekalo to be 0.5 nb as shown in figure 16. 3.8% of $\bar{D}$ decay to $K^+\pi^-$ and almost 100% of Σ_c^+ decay to $\Lambda_c^+\pi^0$. π^0 decays dominantly (98.8%) into $\gamma\gamma$. We want to reconstruct the $\gamma p \rightarrow \bar{D}\Sigma_c^+$ events from the $\bar{D}$ decay products ($K^+\pi^-$) detected in the BigBite spectrometer and at least one photon detected in the NPS as the signature of the π^0 decay. The detection of at least one photon is necessary to reduce the background. Therefore, we use 3.75% as the total branching ratio in the calculation. Based on the equation 11 the

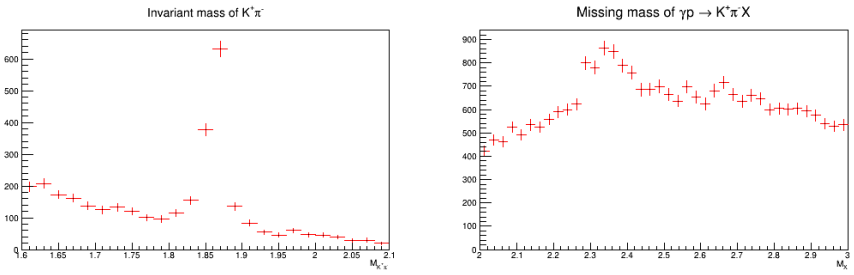

Figure 19: (Left) The invariant mass of $K^+\pi^-$ detected in the BigBite spectrometer. (Right) The reconstructed missing Λ_c^+ invariant mass. The peak is broad but visible enough to impose the required kinematic constraint.

expected event rates per day is

$$N_{\bar{D}\Sigma_c^+} = 1 \times 10^5 \, \epsilon, \tag{13}$$

where the ϵ is the detector acceptance. We then generated 1×10^5 $\gamma p \to \bar{D}\Sigma_c^+$ events and counted the number of events having the K^+ and π^- ($\bar{D} \to K^+\pi^-$) fall in the range of the angles covered by the BigBite spectrometer and at least one photon fall in the range of angles covered by the NPS. cut around Σ_c^+ is applied to further reduce the backgrounds. 467 events are obtained from this method.

Therefore, with the photon flux of $6.2 \times 10^{11}\,\gamma\mathrm{s}^{-1}$ and the acceptance of approximately 0.004% the resulting rate of detected $\gamma p \to \bar{D}\Sigma_c^+$ events is 467 per day.

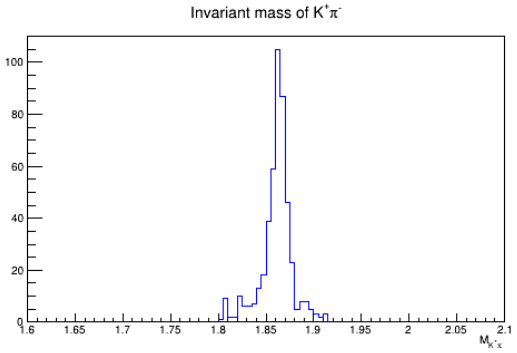

Figure 20: 467 events per day are obtained when K^+ and π^- are detected in the BigBite spectrometer ($\bar{D} \to K^+\pi^-$) and cut around Σ_c^+ mass is applied.

3.3 $\gamma p \rightarrow J/\psi$ reaction

Figure 21 shows the world data for the electro- and photoproduction of J/ψ as compiled in [23], where we can see that the cross section of the J/ψ photoproduction at around threshold is 0.1 nb. Figure 21 shows the world data for the

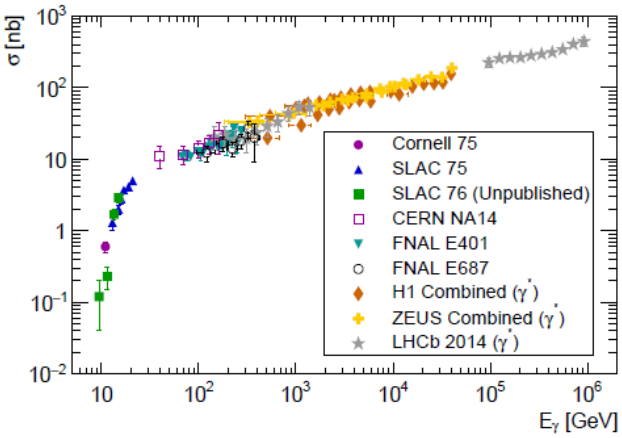

Figure 21: The world data for the electro- and photoproduction of J/ψ. Image source [23].

electro- and photoproduction of J/ψ, where we can see the cross section of the J/ψ photoproduction from threshold to the highest photon energy available at Jefferson Lab. is around 0.1 nb. The branching ratio of the $J/\psi \rightarrow e^+e^-$ decays mode is 5.94%. Hence, based on the equation 11 the expected event rates per day is

$$N_{J\psi} = 3 \times 10^4 \, \epsilon, \tag{14}$$

where the ϵ is the detector acceptance. We then generated 3×10^4 $\gamma p \rightarrow pJ/\psi$ events and counted the number of events having the e^+ and e^- ($J/\psi \rightarrow e^+e^-$) fall in the range of the angles covered by the NPS in coincidence with the detected proton in the BigBite spectrometer. 128 events are obtained from this method.

Therefore, with the photon flux of $6.2 \times 10^{11}\,\gamma s^{-1}$ and the acceptance of approximately 0.004% the resulting rate of detected $\gamma p \rightarrow pJ/\psi$ events is 128 per day.

3.4 $\gamma p \rightarrow D + X$

The open charm photoproduction channels, $\gamma p \rightarrow D + X$ are important to probe the gluon polarization in the nucleon. The cross sections of this production ($\gamma p \rightarrow c\bar{c}$) are experimentally unknown for the Jefferson Lab. energy range. The smallest energy where data are available is $E_\gamma = 20$ GeV.

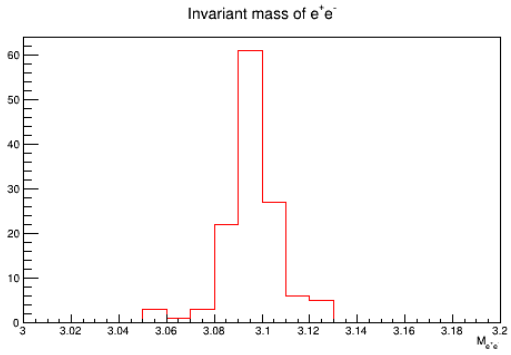

Figure 22: 128 events per day are obtained when e^+ and e^- are detected in the NPS ($J/\psi \rightarrow e^+e^-$) in coincidence with the detected proton in the BigBite spectrometer.

At $E_\gamma = 20$ GeV the excess of $\bar{D}$ over D mesons are observed. The observed excess of $\bar{D}$ mesons is evidence for associated $\gamma p \rightarrow \bar{D}\Lambda_c^+$ production. The contribution of this associated production to the open charm production is estimated to be 71%. If we assume a similar ration all the way down to threshold, we can safely assume that the cross section of the open charm photoproduction near threshold is around 12 nb.

The photoproduction of open charm are also studied at H1 and ZEUS experiments at HERA, where the charm fragmentation fractions were determined. The fragmentation ratio of $f(c \rightarrow D)$ is 0.557 and found to be universal. We want to use the D mesons to tag the open charm production since they are free from the associated production (the D mesons could not be produced from the target remnants). Therefore, the cross section of the $\gamma p \rightarrow c\bar{c} \rightarrow DX$ process is estimated to be 6.7 nb.

The D mesons decay to $K^-\pi^+$ with the branching ratio of 3.93%. If we assume a similar detector acceptance (ϵ) for this process and the exclusive $\gamma p \rightarrow \bar{D}\Lambda_c^+$ channel, the expected event rates per day is 16902 events per day.

4 Beam request and projected results

The measurement of the asymmetries, A are in general performed from two different beam (or target) orientations:

$$A = \frac{1}{\delta}\frac{N^+ - N^-}{N^+ + N^-}, \tag{15}$$

where δ is the degree of polarization, N^+ and N^- are two different orientations of the beam (or target). We request a total of 20 days of beam time for the experiments, consist of 10 days for the circularly-polarized photons (5 days for each orientation) and 10 days for the linearly-polarized photons (5 days for each orientation). If we assume $N^+ = N^-$, the expected number of N^+/N^- for each bin of the observables are summarized in table 4 below

Table 3: The expected event rates for each bin of the observables.

Channels	Observables	$N^+(N^-)$ per 5 days	binning	$N^+(N^-)$ per bin
$\gamma p \to D + X$	A_{LL}	84510	40	2112
$\gamma p \to \bar{D} + \Lambda_c^+$	A_z, Σ	26760	20	1338
$\gamma p \to \bar{D} + \Sigma_c^+$	$A_z\Sigma$	2335	10	233
$\gamma p \to J/\psi p$	Σ, G	640	5	128

The statistical error propagation for the asymmetry is

$$\sigma_A = \frac{1}{\delta}\sqrt{\Big(\frac{\partial A}{\partial N^+}\Big)^2\sigma^2_{N^+} + \Big(\frac{\partial A}{\partial N^-}\Big)^2\sigma^2_{N^-}}. \tag{16}$$

The equation above can be simplified to

$$\sigma_A = \frac{2}{(N^+ + N^-)^2}\sqrt{N^{+2}\sigma^2_{N^-} + N^{-2}\sigma^2_{N^+}} \tag{17}$$

Assuming $N^+ = N^- = N$ and $\sigma_{N^+} = \sigma_{N^-} = \sqrt{N}$, we obtain

$$\sigma_A = \frac{1}{\delta}\frac{1}{2}\sqrt{\frac{2}{N}}. \tag{18}$$

The degree of polarization for the A_{LL}, E and A_z observables is

$$\delta = \delta_{BC}\delta_{TL}, \tag{19}$$

where δ_{BC} is the circular polarization of the photon beam (~ 0.8) and δ_{TL} is the longitudinal polarization of the proton in the target (~ 0.85). The beam asymmetry, Σ requires linear polarization of the photon beam, $\delta = \delta_{BL} \sim 0.5$ and the observable G requires both linear polarization of the photon and longitudinal polarization of the target, $\delta = \delta_{BL}\,\delta_{CL}$. Table 4 shows the estimated statistical uncertainty for all observables that we plan to measure in this experiment.

Table 4: The projected statistical uncertainty for each observable.

Channels	Observables	δ	Statistical uncertainty per bin
$\gamma p \to D + X$	A_{LL}	$\delta_{BC}\delta_{TL}$	0.023
$\gamma p \to D + \Lambda_c^+$	A_z	$\delta_{BC}\delta_{TL}$	0.028
	Σ	δ_{BL}	0.039
$\gamma p \to \bar{D} + \Sigma_c^+$	A_z	$\delta_{BC}\delta_{TL}$	0.068
	Σ	δ_{BL}	0.093
$\gamma p \to J/\psi p$	G	$\delta_{BL}\delta_{TL}$	0.156
	Σ	δ_{BL}	0.125

5 Summary and outlook

We present this letter-of-intent stating our interest to measure various polarization observables in the open charm and charmonium photoproduction near threshold. The major goals of the experiment is to probe the gluon polarization inside the nucleon, investigate the charm-production mechanism and to do a high sensitivity search of the LHCb pentaquark candidates as well as investigating their possible properties (spin and parity). We will also probe the existence of predicted pentaquarks which decay dominantly to $\bar{D}\Lambda_c^+$ and $\bar{D}\Sigma_c^+$.

Several polarization observables ($A_{LL}, A_z, \Sigma, E, G$) are extracted from the reactions: $\gamma p \to D\,X$, $\gamma p \to \bar{D}\Lambda_c^+$, $\gamma p \to \bar{D}\Sigma_c^+$, and $\gamma p \to J/\psi p$. We will use the coherent photon beams with circular and linear polarizations produced from the diamond radiator. We plan to utilize a similar experimental setup as in the approved PR12-17-008 proposal which consist of the Compact Photon Source, the BigBite spectrometer, the Neutral Particle Spectrometer and the UVA/JLab-NH_3 polarized target. We request 20 days of beam time to achieve the projected results and desired sensitivity of the underlying mechanisms of charm production.

We intend this project be part of the CPS and NPS joint effort. With encouragement from the PAC we will write a full proposal with a detailed study of the background, Monte Carlo simulations and technical details about the radiator setup to produce a high quality of coherent beam.

References

[1] M. Gersabeck, arXiv:1502.00032 [Hep-ex] (2015).

[2] J. C. Anjos *et al.* [The Tagged Photon Spectrometer Collaboration], Phys. Rev. Lett. **65**, 20 (1990).

[3] R. G. Arnold, P. E. Bosted, S. E. Rock, spokesperson, "SLAC-PROPOSAL-E161,"(http://www.slac.stanford.edu/exp/e161/charmprp.pdf), Proposal to SLAC (2000).

[4] E. Tomasi-Gustafsson and M. P. Rekalo, Phys. Rev. D **69**, 094015 (2004).

[5] R. Aaij *et al.* [LHCb Collaboration], Phys. Rev. Lett. **115**, 072001 (2015).

[6] D. Aston *et al.*, Phys. Lett. **94B**, 113 (1980).

[7] J. J. Aubert *et al.* [European Muon Collaboration], Nuc. Phys. **B213**, 31 (1983).

[8] J. J. Aubert *et al.* [European Muon Collaboration], Phys. Lett. **167B**, 127 (1986).

[9] K. Abe *et al.* [SLAC Hybrid Facility Photon Collaboration], Phys. Rev. D **33**, 1 (1986).

[10] M. I. Adamovich *et al.* [Photon Emulsion Collaboration], Phys. Lett. B **187**, 1 (1989).

[11] J. C. Anjos *et al.* [The Tagged Photon Spectrometer Collaboration], Phys. Rev. Lett. **62**, 513 (1989).

[12] R. Schumacher, Hall D Collaboration Meeting, https://www.jlab.org/Hall-D/meetings/php2008/talks/r.schumacher.pdf.

[13] S. J. Brodsky *et al.* , Phys. Lett. B **498**, 23-28 (2001).

[14] J. R. Ellis and M. Karliner, Phys. Lett. B **341**, 397 (1995).

[15] J. Pretz *et al.* [COMPASS Collaboration], Nuc. Phys. B **186**, 70-73 (2009).

[16] B. Adeva *et al.* [SMC Collaboration], Phys. Rev. D **58**, 112001 (1998).

[17] A. Airapetian *et al.* [HERMES Collaboration], Phys. Rev. Lett. **84**, 2584 (2000).

[18] I. Nakagawa *et al.* [RHIC Spin Collaboration], EPJ Web of Conferences **141**, 03006 (2017).

[19] R. Aaij *et al.* [LHCb Collaboration], arXiv:1904.03947 [Hep-ph] (2019).

[20] X. Z. Weng *et al.* , arXiv:1904.09891 [Hep-ph] (2019).

[21] C. Fanelli, L. Pentchev, B. Wojtsekhowski, spokesperson, "LOI12-18-001," LOI to JLab PAC 46.

[22] The Hall B Collaboration, "E12-12-001A," Proposal to JLab PAC 45.

[23] Z. -E. Meziani *et al.*, arXiv:1609.00676 [Hep-ex] (2016).

[24] M. Pichowsky, C. Savkli and F. Tabakin , Phys. Rev. C **53**, 593 (1996).

[25] K. Schilling, P. Seyboth and G. E. Wolf, , Nuc. Phys. B **15**, 397 (1970).

[26] X. Y. Wang, X. .R. Chen and Jun He , arXiv:1904.11706 [Hep-ph] (2019).

[27] D. J. Hamilton *et al.*, spokesperson-contact [Hall C Collaboration], "PR12-17-008," Proposal to JLab. PAC 45.

[28] B. Wojtsekhowski *et al.*, A Conceptual Design Study of a Compact Photon Source (CPS) for Jefferson Lab., JLab. internal (2019).

[29] J. D. Kellie *et al.*, A Conceptual Design Study of a Compact Photon Source (CPS) for Jefferson Lab., Nucl. Instrum. Meth. A **545**, 164-180 (2005).